

1 A Non-homogeneous Time Mixed Integer LP

2 Formulation for Traffic Signal Control

3 Iain Guilliard
4 National ICT Australia
5 7 London Circuit
6 Canberra, ACT, Australia
7 iguilliard@nicta.com.au

8 Scott Sanner
9 Oregon State University
10 1148 Kelley Engineering Center
11 Corvallis, OR 97331
12 scott.sanner@oregonstate.edu

13 Felipe W. Trevizan
14 National ICT Australia
15 7 London Circuit
16 Canberra, ACT, Australia
17 felipe.trevizan@nicta.com.au

18 Brian C. Williams
19 Massachusetts Institute of Technology
20 77 Massachusetts Avenue
21 Cambridge, MA 02139
22 williams@csail.mit.edu

23 4516 words + 8 figures + 0 table + 23 citations (Weighted total words: 6516 out of 7000 + 35
24 references)
25 August 1, 2015

1 ABSTRACT

2 We build on the body of work in mixed integer linear programming (MILP) approaches that at-
3 tempt to jointly optimize traffic signal control over an *entire traffic network* (rather than focus on
4 arterial routes) and specifically on improving the scalability of these methods for large urban traf-
5 fic networks. Our primary insight in this work stems from the fact that MILP-based approaches to
6 traffic control used in a receding horizon control manner (that replan at fixed time intervals) need to
7 compute high fidelity control policies only for the early stages of the signal plan; therefore, coarser
8 time steps can be employed to “see” over a long horizon to preemptively adapt to distant platoons
9 and other predicted long-term changes in traffic flows. To this end, we contribute the queue trans-
10 mission model (QTM) which blends elements of cell-based and link-based modeling approaches
11 to enable a non-homogeneous MILP formulation of traffic signal control. We then experiment with
12 this novel QTM-based MILP control in a range of networks demonstrating the improved scalabil-
13 ity possible with non-homogeneous time steps in comparison to the best homogeneous time step.
14 Our experiments also provide near-optimal traffic control policies for larger horizons and larger
15 networks than shown in previous implementations of MILP-based traffic signal control.

16 Using 204 words up to here. Maximum is 250 words.

1 INTRODUCTION

2 As cities rapidly grow in population while urban traffic infrastructure often adapts at a slower pace,
 3 it is critical to maximize capacity and throughput of existing road infrastructure through optimized
 4 traffic signal control. Unfortunately, many large cities still use some degree of *fixed-time* control
 5 (e.g., Toronto (1)) even if they also use *actuated* or *adaptive* control methods such as SCATS (2)
 6 or SCOOT (3). However, there is further opportunity to improve traffic signal control even beyond
 7 adaptive methods through the use of *optimized* controllers as evidenced in a variety of approaches
 8 ranging from mixed integer (linear) programming (4, 5, 6, 7, 8, 9) to heuristic search (10, 11) to
 9 scheduling (12) to reinforcement learning (1). While such optimized controllers hold the promise
 10 of maximizing existing infrastructure capacity by finding more complex (and potentially closer to
 11 optimal) jointly coordinated intersection policies than arterially-focused master-slave approaches
 12 such as SCATS and SCOOT, such optimized methods are computationally demanding and either
 13 (a) do not guarantee jointly optimal solutions over a large intersection network (often because they
 14 only consider coordination of neighboring intersections or arterial routes) or (b) fail to scale to
 15 large intersection networks simply for computational reasons (which is the case for many mixed
 16 integer programming approaches).

17 In this work, we build on the body of work in mixed integer linear programming (MILP) ap-
 18 proaches that attempt to jointly optimize traffic signal control over an *entire traffic network* (rather
 19 than focus on arterial routes) and specifically on improving the scalability of these methods for
 20 large urban traffic networks. In our investigation of existing approaches in this vein, namely exem-
 21 plar methods in the spirit of (6, 8, 9) that use a (modified) cell transmission model (CTM) (13, 14)
 22 for their underlying prediction of traffic flows, we remark that a major drawback is the CTM-
 23 imposed requirement to choose a predetermined homogeneous (and often necessarily small) time
 24 step for reasonable modeling fidelity. This need to model large number of CTM cells with a small
 25 time step leads to MILPs that are exceedingly large and intractable to solve.

26 Our primary insight in this work stems from the fact that MILP-based approaches to traffic
 27 control used in a receding horizon control manner (that replan at fixed time intervals) need to
 28 compute high fidelity control policies only for the early stages of the signal plan; therefore, coarser
 29 time steps can be employed to “see” over a long horizon to preemptively adapt to distant platoons
 30 and other predicted long-term changes in traffic flows. This need for non-homogeneous control
 31 in turn spawns the need for an additional innovation: we require a traffic flow model that permits
 32 non-homogeneous time steps and properly models the travel time delay between lights. To this
 33 end, we might consider CTM extensions such as the variable cell length CTM (15), stochastic
 34 CTM extensions (16, 17), extensions for better modeling freeway-urban interactions (18) including
 35 CTM hybrids with link-based models (19), asymmetric CTMs for better handling flow imbalances
 36 in merging roads (20), the situational CTM for better modeling of boundary conditions (21), and
 37 the lagged CTM for improved modeling of the flow density relation (22). However, despite the
 38 widespread varieties of the CTM and the usage of the CTM (23) for a range of applications, there
 39 seems to be no extension that permits non-homogeneous time steps as required in our novel MILP-
 40 based control approach.

41 For this reason, as a major contribution of this work to enable our non-homogeneous
 42 time MILP-based model of joint intersection control, we contribute the queue transmission model
 43 (QTM) which blends elements of cell-based and link-based modeling approaches with the follow-
 44 ing key benefits:

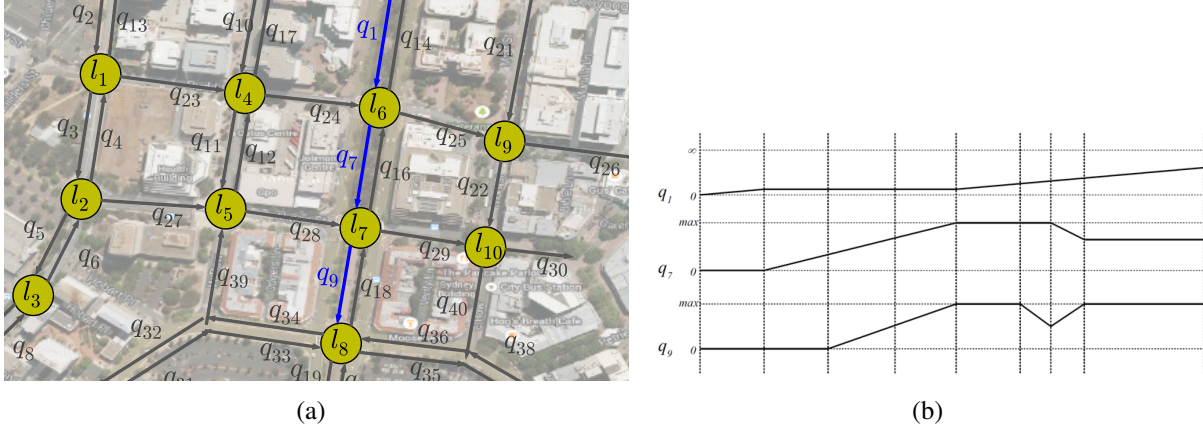


FIGURE 1 (a) Example of how a real network is modeled using QTM. (b) Volume of traffic in different queues as a function of non-homogeneous discretized time.

- unlike previous joint intersection control work (6, 8, 9), it is inherently intended for *non-homogeneous* time steps that can be used for control over large horizons,
- any length of roadway with no merges or diverges can be modeled as a single queue leading to compact models of large traffic networks thus maintaining relatively compact MILPs for large traffic networks (i.e., large numbers of cells are not required between intersections), and
- it accurately models fixed travel time delays critical to green wave coordination as in (4, 5, 7) through the use of a non-first order Markovian update model and combines this with the more global intersection signal optimization approach of (6, 8, 9).

In the remainder of this paper, we first formalize our novel QTM model of traffic flow with non-homogeneous time steps and show how to encode it as a linear program for simulating traffic. We proceed to allow the traffic signals to become discrete variables subject to a delay minimizing optimization objective and standard cycle and phase time constraints leading to our final MILP formulation of traffic signal control. We then experiment with this novel QTM-based MILP control in a range of networks demonstrating the improved scalability possible with non-homogeneous time steps in comparison to the best homogeneous time step. These experiments also provide near-optimal traffic control policies for larger horizons and larger networks than shown in previous implementations of MILP-based traffic signal control.

THE QUEUE TRANSMISSION MODEL

A Queue Transmission Model (QTM) is the tuple $(\mathcal{Q}, \mathcal{L}, \vec{\Delta t}, \mathbf{I})$, where \mathcal{Q} and \mathcal{L} are, respectively, the set of queues and lights; $\vec{\Delta t}$ is a vector of size N representing the discretization of the simulation horizon $[0, T]$ and the duration in seconds of the n -th time interval is denoted as Δt_n ; and \mathbf{I} is a matrix $|\mathcal{Q}| \times T$ in which $I_{i,n}$ represents the flow of cars requesting to enter queue i from the outside of the network at time n .

A **traffic light** $\ell \in \mathcal{L}$ is defined as the tuple $(\Psi_\ell^{\min}, \Psi_\ell^{\max}, \mathcal{P}_\ell, \vec{\Phi}_\ell^{\min}, \vec{\Phi}_\ell^{\max})$, where:

- \mathcal{P}_ℓ is the set of phases of ℓ ;

- Ψ_ℓ^{\min} (Ψ_ℓ^{\max}) is the minimum (maximum) allowed cycle time for ℓ ; and
- $\vec{\Phi}_\ell^{\min}$ ($\vec{\Phi}_\ell^{\max}$) is a vector of size $|\mathcal{P}_\ell|$ and $\Phi_{\ell,k}^{\min}$ ($\Phi_{\ell,k}^{\max}$) is the minimum (maximum) allowed time for phase $k \in \mathcal{P}_\ell$.

A **queue** $i \in \mathcal{Q}$ represents a segment of road that vehicles traverse at free flow speed; once traversed, the vehicles are vertically stacked in a stop line queue. Formally, a queue i is defined by the tuple $(Q_i, T_i^{\text{prop}}, F_i^{\text{out}}, \vec{F}_i, \vec{Pr}_i, \mathcal{Q}_i^{\mathcal{P}})$ where:

- Q_i is the maximum capacity of i ;
- T_i^{prop} is the time required to traverse i and reach the stop line;
- F_i^{out} represents the maximum traffic flow from i to the outside of the modeled network;
- \vec{F}_i and \vec{Pr}_i are vectors of size $|\mathcal{Q}|$ and their j -th entry (i.e., $F_{i,j}$ and $Pr_{i,j}$) represent the maximum flow from queue i to j and the turn probability from i to j ($\sum_{j \in \mathcal{Q}} Pr_{i,j} = 1$), respectively; and
- $\mathcal{Q}_i^{\mathcal{P}}$ denotes the set of traffic light phases controlling the outflow of queue i .

Differently than CTM (8, 13), QTM does not assume that $\Delta t_n = T_i^{\text{prop}}$ for all n , that is, the QTM can represent non-homogeneous time intervals (Figure 1(b)). The only requirement over Δt_n is that no traffic light maximum phase time is smaller than any Δt_n since phase changes occur only between time intervals; formally, $\Delta t_n \leq \min_{\ell \in \mathcal{L}, k \in \mathcal{P}_\ell} \Phi_{\ell,k}^{\max}$ for all $n \in \{1, \dots, N\}$.

Traffic Flow Simulation with QTM

In this section, we present how to simulate traffic flow using QTM and non-homogeneous time intervals Δt . We assume for the remainder of this section that a *valid* control plan for all traffic lights is fixed and given as parameter; formally, for all $\ell \in \mathcal{L}$, $k \in \mathcal{P}_\ell$, and interval $n \in \{1, \dots, N\}$, the binary variable $p_{\ell,k,n}$ is known a priori and indicates if phase k of light ℓ is active (i.e., $p_{\ell,k,n} = 1$) or not on interval n .

We represent the problem of finding the flow between queues as a Linear Program (LP) over the following variables defined for all interval $n \in \{1, \dots, N\}$ and queues i and j :

- $q_{i,n} \in [0, Q_i]$: traffic volume waiting in the stop line of queue i at the beginning of interval n ;
- $f_{i,n}^{\text{in}} \in [0, I_{i,n}]$: inflow to the network via queue i during interval n ;
- $f_{i,n}^{\text{out}} \in [0, F_i^{\text{out}}]$: outflow from the network via queue i during interval n ; and
- $f_{i,j,n} \in [0, F_{i,j}]$: flow from queue i into queue j during interval n .

The maximum traffic flow from queue i to queue j is enforced by constraints (C1) and (C2). (C1) ensures that only the fraction $Pr_{i,j}$ of the total internal outflow of i goes to j , and (C2) forces

- 1 the flow from i to j to be zero if all phases controlling i are inactive (i.e., $p_{\ell,k,n} = 0$ for all $k \in \mathcal{Q}_i^P$).
 2 If more than one phase $p_{\ell,k,n}$ is active, then (C2) is subsumed by the domain upper bound of $f_{i,j,n}$.

$$3 \quad f_{i,j,n} \leq \Pr_{i,j} \sum_{k=1}^{|\mathcal{Q}|} f_{i,k,n} \quad (C1)$$

$$4 \quad f_{i,j,n} \leq F_{i,j} \sum_{p_{\ell,k,n} \in \mathcal{Q}_i^P} p_{\ell,k,n} \quad (C2)$$

- 6 To simplify the presentation of remainder of the LP, we define the helper variables $q_{i,n}^{\text{in}}$ (C3),
 7 $q_{i,n}^{\text{out}}$ (C4), and t_n (C5) to represent the volume of traffic to enter and leave queue i during interval n ,
 8 and the time elapsed since the beginning of the simulation until the end of interval Δt_n .

$$9 \quad q_{i,n}^{\text{in}} = \Delta t_n (f_{i,n}^{\text{in}} + \sum_{j=1}^{|\mathcal{Q}|} f_{j,i,n}) \quad (C3)$$

$$10 \quad q_{i,n}^{\text{out}} = \Delta t_n (f_{i,n}^{\text{out}} + \sum_{j=1}^{|\mathcal{Q}|} f_{i,j,n}) \quad (C4)$$

$$11 \quad t_n = \sum_{x=1}^n \Delta t_x \quad (C5)$$

- 13 In order to account for the misalignment of the different Δt and T_i^{prop} , we need to find the
 14 volume of traffic that entered queue i between two arbitrary points in time x and y ($x \in [0, T]$,
 15 $y \in [0, T]$, and $x < y$), i.e., x and y might not coincide with any t_n for $n \in \{1, \dots, N\}$. This
 16 volume of traffic, denoted as $V_i(x, y)$, is obtained by integrating $q_{i,n}^{\text{in}}$ over $[x, y]$ and is defined in
 17 (1) where m and w are the index of the time intervals s.t. $t_m \leq x < t_{m+1}$ and $t_w \leq y < t_{w+1}$.
 18 Because the QTM dynamics is piecewise linear, $q_{i,n}^{\text{in}}$ is a step function w.r.t. time and this integral
 19 reduces to the sum of $q_{i,n}^{\text{in}}$ over the intervals contained in $[x, y]$ and the appropriate fraction of $q_{i,m}^{\text{in}}$
 20 and $q_{i,w}^{\text{in}}$ representing the misaligned beginning and end of $[x, y]$.

$$21 \quad V_i(x, y) = (t_{m+1} - x) \frac{q_{i,m}^{\text{in}}}{\Delta t_m} + \left(\sum_{k=m+1}^{w-1} q_{i,k}^{\text{in}} \right) + (y - t_w) \frac{q_{i,w}^{\text{in}}}{\Delta t_w} \quad (1)$$

- 22 Using these helper variables, (C6) represents the flow conservation principle for queue i
 23 where $V_i(t_{n-1} - T_i^{\text{prop}}, t_n - T_i^{\text{prop}})$ is the volume of cars that reached stop line during Δt_n . Since
 24 $\vec{\Delta t}$ and T_i^{prop} for all queues are known a priori, the indexes m and w used by V_i can be pre-
 25 computed in order to encode (1); moreover, (C6) represents a non-first order Markovian update
 26 because the update considers the previous $w - m$ time steps. To insure that the total volume of
 27 traffic traversing i (i.e., $V_i(t_n - T_i^{\text{prop}}, t_n)$) and waiting at the stop line does not exceed the capacity
 28 of the queue, we apply (C7).

$$29 \quad q_{i,n} = q_{i,n-1} - q_{i,n-1}^{\text{out}} + V_i(t_{n-1} - T_i^{\text{prop}}, t_n - T_i^{\text{prop}}) \quad (C6)$$

$$30 \quad V_i(t_n - T_i^{\text{prop}}, t_n) + q_{i,n} \leq Q_i \quad (C7)$$



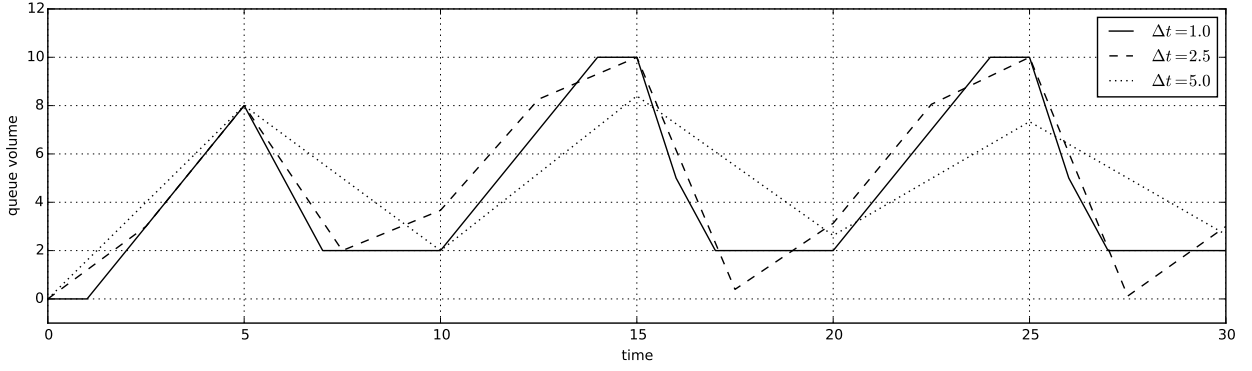
FIGURE 2 Cumulative arrival (blue) and departure (green) curves, and the resulting delay curve (red). The departure curve is maximized by the objective function (O1), which has the same effect as minimizing the delay curve.

As with MILP formulations of CTM (e.g. Lin and Wang (8)), QTM is also susceptible to *withholding traffic*, i.e., the optimizer might prevent cars from moving from i to j even though the associated traffic phase is active and j is not full. We address this issue through our objective function (O1) by maximizing the total outflow $q_{i,n}^{\text{out}}$ (i.e., both internal and external outflow) of i plus the inflow $f_{i,n}^{\text{in}}$ from the outside of the network to i . This quantity is weighted by the remaining time until the end of the simulation horizon T to force the optimizer to allow as much traffic volume as possible into the network and move traffic to the outside of the network as soon as possible.

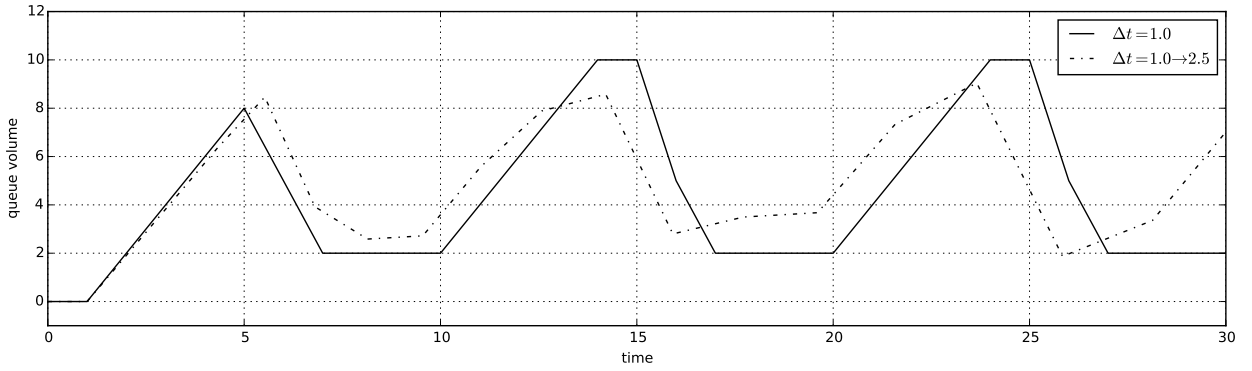
$$\max \sum_{n=1}^N \sum_{i=1}^{|Q|} (T - t_n + 1) (q_{i,n}^{\text{out}} + f_{i,n}^{\text{in}}) \quad (\text{O1})$$

The objective (O1) corresponds to minimizing delay in CTM models, e.g., (O1) is equivalent to the objective function (O3) in Lin and Wang (8) for their parameters $\alpha = \beta = 1$. Figure 2 depicts this equivalence using the cumulative number of cars entering and leaving a network as a function of time. The delay experienced by the vehicles travelling through this network (red curve in Figure 2) equals the horizontal difference at each point between the cumulative departure and arrival curves (less the free flow travel time through the network). Maximizing $q_{i,n}^{\text{out}}$ weighted by $(T - t_n + 1)$ in (O1) is the same as forcing the departure curve to be as close as possible to the arrival curve as early as possible; therefore, the area between arrival and departure is minimized, which in turn minimizes the delay.

To illustrate the representation tradeoff offered by non-homogeneous time intervals, we simulate a fixed signal control plan derived for homogeneous $\Delta t_n = 1\text{s}$ (ground truth) using different discretizations. Figure 3(a) shows the approximation of the ground truth using homogeneous $\Delta t = 2.5$ and $\Delta t = 5.0$, and Figure 3(b) using non-homogeneous time intervals that linearly increases from 1s to 2.5s, i.e., $\Delta t_n \approx 0.0956n + 0.9044$ for $n \in \{1, \dots, 17\}$. As Figure 3(a) shows, large time steps can be rough approximations of the ground truth. Non-homogeneous discretization (Figure 3(b)) exploit this fact to provide a good approximation in the initial time steps and progressively decrease precision for points far in the future.



(a)



(b)

FIGURE 3 Approximations of a queue volume obtained using homogeneous $\Delta t = 1$ s using: (a) homogeneous $\Delta t = 2.5$ s and 5s; and (b) non-homogeneous $\Delta t_n \approx 0.0956n + 0.9044$ for $n \in \{1, \dots, 17\}$.

1 TRAFFIC CONTROL WITH QTM AS AN MILP

2 In this section, we remove the assumption that a valid control plan for all traffic lights is given
 3 and extend the LP (O1, C1–C7) to an Mixed-Integer LP (MILP) that also computes the optimal
 4 control plan. Formally, for all $\ell \in \mathcal{L}$, $k \in \mathcal{P}_\ell$, and interval $n \in \{1, \dots, N\}$, the phase activation
 5 parameter $p_{\ell,k,n} \in \{0, 1\}$ becomes a free variable to be optimized. In order to obtain a valid control
 6 plan, we enforce that one phase of traffic light ℓ is always active at any interval n (C8) and that
 7 phase changes happen sequentially (C9), i.e., if phase k was active during interval $n - 1$ and has
 8 become inactive in interval n , then phase $k + 1$ must be active in interval n . (C9) assumes that
 9 $k + 1$ equals 1 if $k = |\mathcal{P}_\ell|$.

$$10 \quad \sum_{k=1}^{|\mathcal{P}_\ell|} p_{\ell,k,n} = 1 \quad (C8)$$

$$11 \quad p_{\ell,k,n-1} \leq p_{\ell,k,n} + p_{\ell,k+1,n} \quad (C9)$$

12
 13 Next, we enforce the minimum and maximum phase durations (i.e., $\Phi_{\ell,k}^{\min}$ and $\Phi_{\ell,k}^{\max}$) for
 14 each phase $k \in \mathcal{P}_\ell$ of traffic light ℓ . To encode these constraints, we use the helper variable

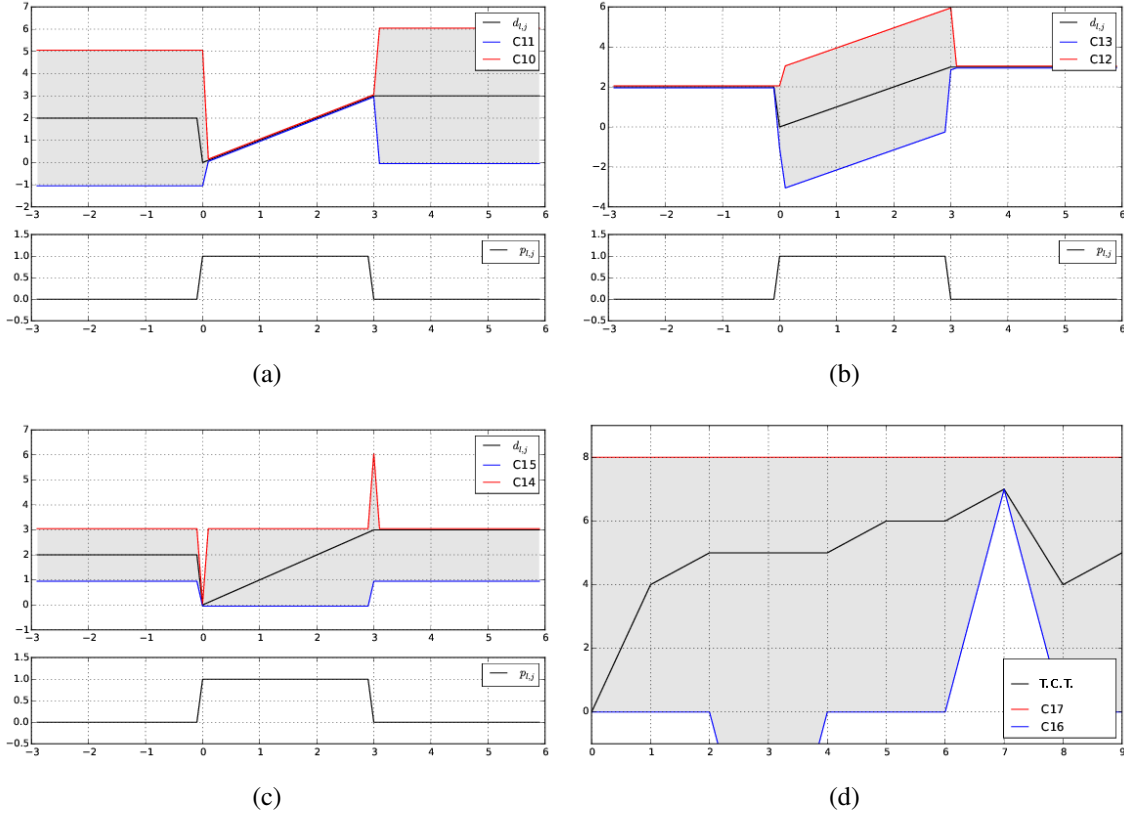


FIGURE 4 Visualization of constraints (C10–C17) for a traffic light ℓ as a function of time. (a–c) present, pairwise, the constraints (C10–C15) for phase k ($d_{\ell,k,n}$ as the black line) and the activation variable $p_{\ell,k,n}$ in the small plot. (d) presents the constraints for the cycle time of ℓ (C16 and C17), where T.C.T. is the total cycle time and is the left hand side of both constraints. For this example, $\Phi_{\ell,k}^{\min} = 1$, $\Phi_{\ell,k}^{\max} = 3$, $\Psi_{\ell}^{\min} = 7$, and $\Psi_{\ell}^{\max} = 8$.

1 $d_{\ell,k,n} \in [0, \Phi_{\ell,k}^{\max}]$, defined by constraints (C10–C14), that: (i) holds the elapsed time since the
2 start of phase k when $p_{\ell,k,n}$ is active (C10,C11); (ii) is constant and holds the duration of the last
3 phase until the next activation when $p_{\ell,k,n}$ is inactive (C12,C13); and (iii) is restarted when phase k
4 changes from inactive to active (C14). Notice that (C10–C14) employs the *big-M* method to turn
5 the cases that should not be active into subsumed constraints based on the value of $p_{\ell,k,n}$. We
6 use $\Phi_{\ell,k}^{\max}$ as our large constant since $d_{\ell,k,n} \leq \Phi_{\ell,k}^{\max}$ and $\Delta t_n \leq \Phi_{\ell,k}^{\max}$ by assumption (Section 2.1).
7 Similarly, constraint (C15) ensures the minimum phase time of k and is not enforced while k is
8 still active. Figures 4(a) to 4(c) present an example of how (C10–C15) work together as a function
9 of the time n for $d_{\ell,k,n}$; the domain constraint $0 \leq d_{\ell,k,n} \leq \Phi_{\ell,k}^{\max}$ for all $n \in \{1, \dots, N\}$ is omitted

for clarity.

$$d_{\ell,k,n} \leq d_{\ell,k,n-1} + \Delta t_{n-1} p_{\ell,k,n-1} + \Phi_{\ell,k}^{\max}(1 - p_{\ell,k,n-1}) \quad (\text{C10})$$

$$d_{\ell,k,n} \geq d_{\ell,k,n-1} + \Delta t_{n-1} p_{\ell,k,n-1} - \Phi_{\ell,k}^{\max}(1 - p_{\ell,k,n-1}) \quad (\text{C11})$$

$$d_{\ell,k,n} \leq d_{\ell,k,n-1} + \Phi_{\ell,k}^{\max} p_{\ell,k,n-1} \quad (\text{C12})$$

$$d_{\ell,k,n} \geq d_{\ell,k,n-1} - \Phi_{\ell,k}^{\max} p_{\ell,k,n-1} \quad (\text{C13})$$

$$d_{\ell,k,n} \leq \Phi_{\ell,k}^{\max}(1 - p_{\ell,k,n} + p_{\ell,k,n-1}) \quad (\text{C14})$$

$$d_{\ell,k,n} \geq \Phi_{\ell,k}^{\min}(1 - p_{\ell,k,n}) \quad (\text{C15})$$

Lastly, we constrain the sum of all the phase durations for light ℓ to be within the cycle time limits Ψ_{ℓ}^{\min} (C16) and Ψ_{ℓ}^{\max} (C17). In both (C16) and (C17), we use the duration of phase 1 of ℓ from the previous interval $n - 1$ instead of the current interval n because (C14) forces $d_{\ell,1,n}$ to be 0 at the beginning of each cycle; however, from the previous end of phase 1 until $n - 1$, $d_{\ell,1,n-1}$ holds the correct elapse time of phase 1. Additionally, (C16) is enforced right after the end of the each cycle, i.e., when its first phase is changed from inactive to active. The value (C16) and (C17) over time for a traffic light ℓ is illustrated in Figure 4(d).

$$d_{\ell,1,n-1} + \sum_{k=2}^{|\mathcal{P}_{\ell}|} d_{\ell,k,n} \geq \Psi_{\ell}^{\min}(p_{k,1,n} - p_{k,1,n-1}) \quad (\text{C16})$$

$$d_{\ell,1,n-1} + \sum_{k=2}^{|\mathcal{P}_{\ell}|} d_{\ell,k,n} \leq \Psi_{\ell}^{\max} \quad (\text{C17})$$

The MILP that encodes the problem of finding the optimal traffic control plan in a QTM network is defined by (O1, C1–C17).

EMPIRICAL EVALUATION

In this section we compare the solutions for traffic networks modeled as a QTM using homogeneous and non-homogeneous time intervals in two aspects: the quality of the solution and convergence to the optimal solution. We compare the quality of solutions based on the total travel time and we also consider the third quartile and maximum of the observed delay distribution. Our hypotheses are: (i) the quality of the non-homogeneous solutions is at least as good as the homogeneous ones when the number of time intervals N is fixed; and (ii) the non-homogeneous approach requires less time intervals (i.e., smaller N) than the homogeneous approach to converge to the optimal solution. In the remainder of this section, we present the traffic networks considered in the experiments, our methodology, and the results.

Networks

We consider three networks of increasing complexity (Figure 5): an avenue crossed by three side streets; a 2-by-3 grid; and a 3-by-3 grid with a diagonal avenue. The queues receiving cars from outside of the network are marked in Figure 5 and we refer to them as input queues. The maximum queue capacity (Q_i) is 60 cars for non-input queues and infinity for input queues to prevent interruption of the input demand due to spill back from the stop line. The traversal time of each queue i (T_i^{prop}) is set at 9s (a distance of about 100m with a free flow speed of 50km/h). Flows are



FIGURE 5 (a–c) Networks used to evaluate the QTM performance. (d) Demand profile of the queues marked as \diamond , \clubsuit , and \spadesuit for our experiments.

1 defined from the head of each queue i into the tail of the next queue j ; there is no turning traffic
2 ($\Pr_{i,j} = 1$), and the maximum flow rate between queues, $F_{i,j}$, is set at 5 cars/s. All traffic lights
3 have two phases, north-south and east-west, and lights 2, 4 and 6 of network 3 have the additional
4 northeast-southwest phase to control the diagonal avenue. For networks 1 and 2, $\Phi_{\ell,k}^{\min}$ is 1s, $\Phi_{\ell,k}^{\max}$
5 is 3s, Ψ_{ℓ}^{\min} is 2s, and Ψ_{ℓ}^{\max} is 6s, for all traffic light ℓ and phase k . For network 3, $\Phi_{\ell,k}^{\min}$ is 1s and
6 $\Phi_{\ell,k}^{\max}$ is 6s for all ℓ and k ; and Ψ_{ℓ}^{\min} is 2s and Ψ_{ℓ}^{\max} is 12s for all lights ℓ except for lights 2, 4 and
7 6 (i.e., lights also used by the diagonal avenue) in which Ψ_{ℓ}^{\min} is 3s and Ψ_{ℓ}^{\max} is 18s.

8 Experimental Methodology

9 For each network, a constant background level traffic is injected in the network in the first 55s to
10 allow the solver to settle on a stable policy. Then a spike in demand is introduced in the queues
11 marked as \spadesuit (Figure 5) from time 55s to 70s to trigger a policy change. From time 70s to 85s,
12 the demand is returned to the background level, and then reduced to zero for all input queues. We
13 extend the problem horizon T until all cars have left the network. By clearing the network, we can
14 easily measure the total travel time for all the traffic as the area between the cumulative arrival and
15 departure curves measured at the boundaries of the network. The background level for the input
16 queues are 1, 4 and 2 cars/s for queues marked as \diamond , \clubsuit and \spadesuit (Figure 5(d)), respectively; and



FIGURE 6 Receding horizon control. In this example, the problem horizon T is 40s. The major frames are discretized in 12 time intervals ($N = 12$) and they span 15s and 30s for homogeneous and non-homogeneous discretizations, respectively.

1 during the high demand period, the queues ♠ receive 4 cars/s.

2 For both homogeneous and non-homogeneous intervals, we use the MILP QTM formula-
 3 tion (Section 3) in a receding horizon manner: a control plan is computed for a pre-defined horizon
 4 (smaller than T) and only a prefix of this plan is executed before generating a new control plan.
 5 Figure 6 depicts our receding horizon approach and we refer to the planning horizon as a major
 6 frame and its executable prefix as a minor frame. Notice that, while the plan for a minor frame is
 7 being executed, we can start computing the solution for the next major frame based on a forecast
 8 model.

9 To perform a fair comparison between the homogeneous and non-homogeneous discretiza-
 10 tions, we fix the size of all minor frames to 10s and force it to be discretized in homogeneous
 11 intervals of 0.25s. For the homogeneous experiments, Δt is kept at 0.25s throughout the major
 12 frame; therefore, given N , the major frame size equals $N/4$ seconds for the homogeneous ap-
 13 proach. For the non-homogeneous experiments, Δt linearly increases from 0.25s at the end of
 14 the minor frame to 1.0s at the end of the major frame; therefore, the major frame size used by
 15 the non-homogeneous approach is $10.375 + 0.625(N - 40)$ seconds for a given $N > 40$. Once
 16 we have generated a series of minor frames, we concatenate them into a single plan and simulate
 17 the flow through the network using the QTM LP formulation with a fixed (homogeneous) Δt of
 18 0.25s. We also compare both receding horizon approaches against the optimal solution obtained
 19 by computing a single control plan for the entire control horizon (i.e., $[0, T]$) using a fixed Δt of
 20 0.25s.

21 For all our experiments, we used GurobiTM as MILP solver with 12 threads on a 3.1GHz
 22 AMD OpteronTM 4334 processor with 12 cores. We limit the MIP gap accuracy to 0.1% and the
 23 time cutoff for solving a major frame to 3000s for the receding horizon approaches and unbounded
 24 for the optimal plan. All our results are averaged over five runs to account for Gurobi's stochastic
 25 strategies.

26 Results

27 Figures 7(a), 7(c) and 7(e) show, for each network, the increase in the total travel time w.r.t. the
 28 optimal solution as a function of N . As we hypothesized, the non-homogeneous discretization re-
 29 quires less time intervals (i.e., smaller N) to obtain a solution with the same total travel time. This
 30 is important because the size of the MILP, including the number of binary variables, scales linearly
 31 with N ; therefore, the non-homogeneous approach can scale up better than the homogeneous one

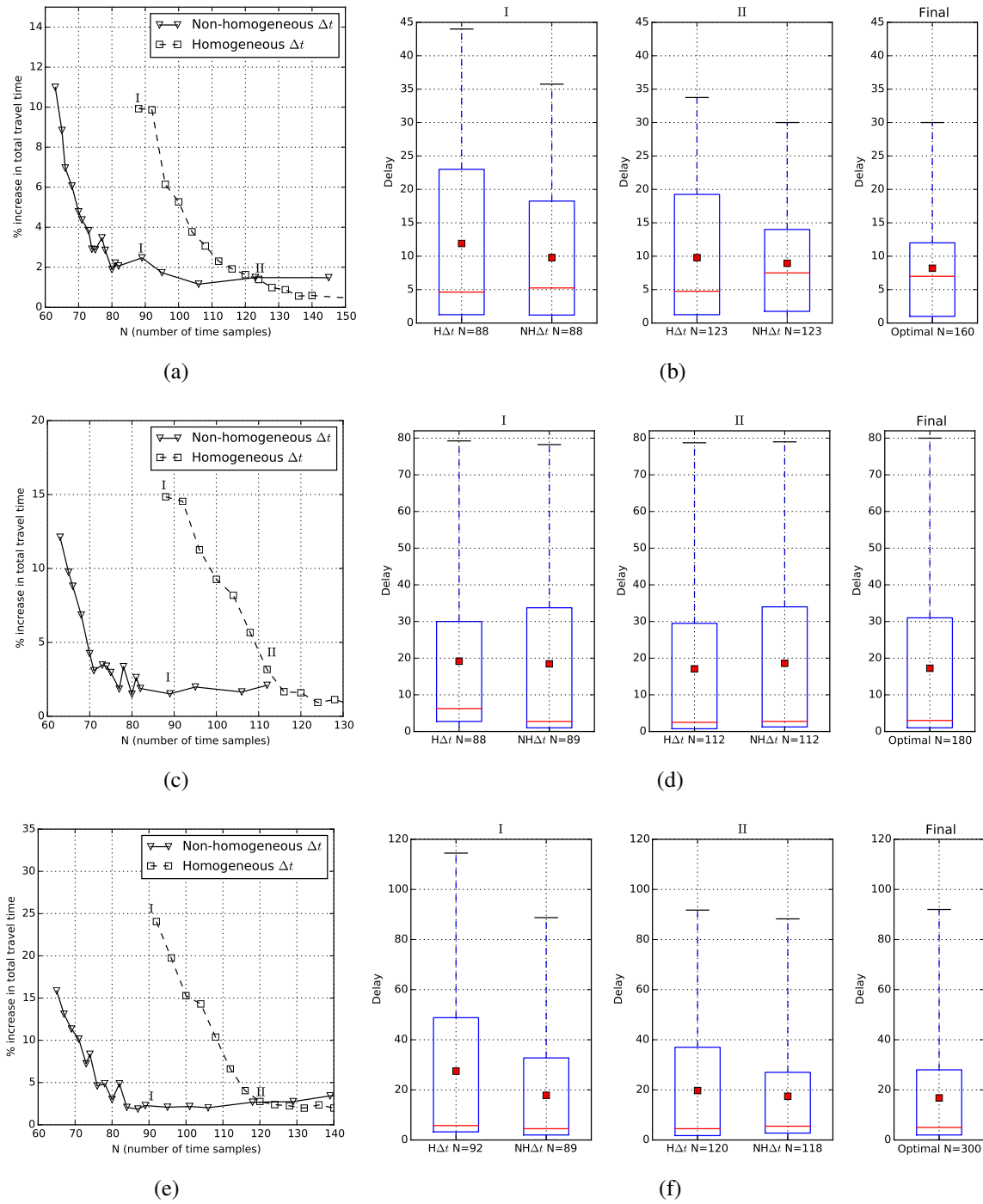


FIGURE 7 Increase in the total travel time w.r.t. the optimal solution as a function of N (Figures a, c, and e) and distribution of the total delay of each car for different values of N (Figures b, d, and f). For each row, the roman numeral on top of the box plots corresponds to point the travel time plot marked with the same numeral. The mean of the total delay is presented as a red square in box plots. Plots in the i -th row correspond to the results for the i -th network in Figure 5.

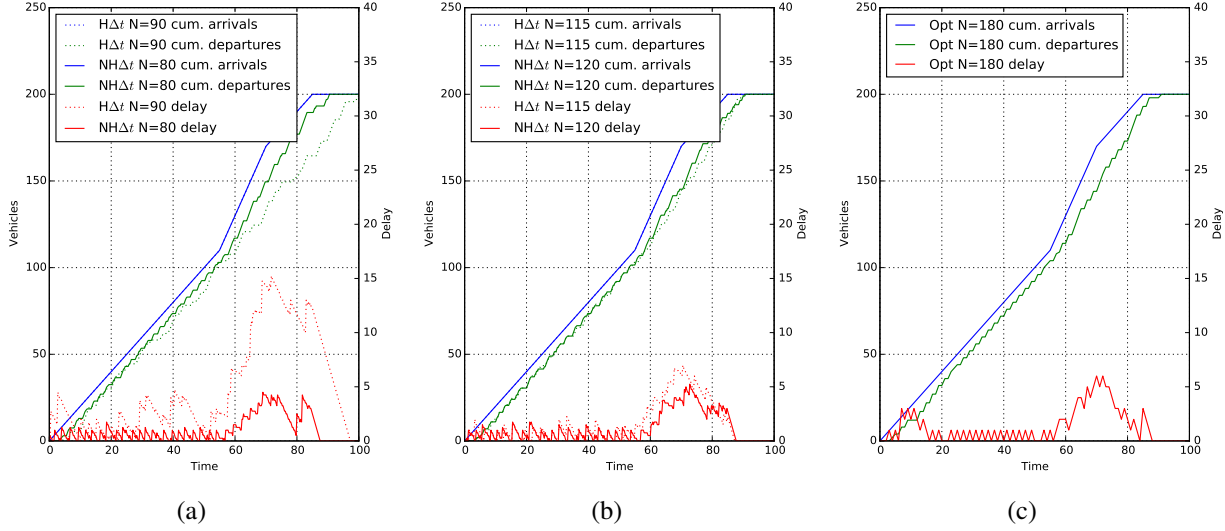


FIGURE 8 Cumulative arrival and departure curves and delay for queue 1 in the 2-by-3 network (Figure 5(b)). The value of N in plots (a) and (b) corresponds, respectively, to the convergence point of the non-homogeneous and homogeneous approaches (Figure 7(c)). (c) presents the same curves for the optimal solution.

(e.g., Figure 7(e)). Also, for homogeneous and non-homogeneous discretizations, finding the optimal solution of major frames with large N might require more time than our imposed 3000s time cutoff and, in this case, Gurobi returns a feasible control plan that is far from optimal. The effect in the total travel time of these poor solutions can be seen in Figure 7(e) for $N > 120$.

The distribution of the total delay observed by each car while traversing the network is shown in Figures 7(b), 7(d) and 7(f). Each group of box plots represents a different value of N : when the non-homogeneous Δt first converges; when the homogeneous Δt first converges; and the optimum solution itself. In all networks, the quality of the solution obtained using non-homogeneous Δt is better or equal than using homogeneous Δt for fixed N in both the total travel time and *fairness*, i.e., smaller third quartile and maximum delay.

To further illustrate the differences between homogeneous and non-homogeneous discretizations, Figure 8 shows the cumulative arrival and departure curves and the how delay evolves over time for q_1 of network 2 (Figure 5(b)). In Figure 8(a), the comparison is done when non-homogeneous Δt first converges (i.e., point I in Figure 7(c)) and for this value of N , the major frame size in seconds of the non-homogeneous approach is 19.125s longer than the homogeneous one. This allows the MILP solver to “see” 19s further in the future when using non-homogeneous discretization and find a coordinated signal policy along the avenue to dissipate the extra traffic that arrives at time 55s. The shorter major frame of the homogeneous discretization does not allow the solver to adapt this far in advance and its delay observed after 55s is much larger than the non-homogeneous one. Once the homogeneous Δt has converged (Figure 8(b)), it is also able to anticipate the increased demand and adapt well in advance and both approaches generate solutions close to optimum (Figure 8(c)).

CONCLUSION

In this paper, we showed how to formulate a novel queue transmission model (QTM) model of traffic flow with non-homogeneous time steps as a linear program. We then proceeded to allow the traffic signals to become discrete variables subject to a delay minimizing optimization objective and standard traffic signal constraints leading to a final MILP formulation of traffic signal control. We experimented with this novel QTM-based MILP control in a range of networks and demonstrated that by exploiting the non-homogeneous time steps supported by the QTM, we are able to scale the model up to larger networks whilst maintaining the same quality of a homogeneous solution using more binary variables. Altogether, this work represents a major step forward in the scalability of MILP-based jointly optimized traffic signal control via the use of a non-homogeneous traffic models and thus helps pave the way for fully optimized joint urban traffic signal controllers as an improved successor technology to existing signal control methods.

ACKNOWLEDGMENT

This work is part of the Advanced Data Analytics in Transport programme, and supported by National ICT Australia (NICTA) and NSW Trade&Investment. NICTA is funded by the Australian Government through the Department of Communications and the Australian Research Council through the ICT Centre of Excellence Program. NICTA's role is to pursue potentially economically significant ICT related research for the Australian economy. NSW Trade&Investment is the business development agency for the State of New South Wales.

REFERENCES

- [1] El-Tantawy, S., B. Abdulhai, and H. Abdelgawad, Multiagent reinforcement learning for integrated network of adaptive traffic signal controllers (MARLIN-ATSC): methodology and large-scale application on downtown toronto. *Intelligent Transportation Systems, IEEE Transactions on*, Vol. 14, No. 3, 2013, pp. 1140–1150.
- [2] Sims, A. G. and K. W. Dobinson, SCAT—The Sydney co-ordinated adaptive traffic system: Philosophy and benefits. *IEEE Transactions on Vehicular Technology*, Vol. 29, 1980.
- [3] Hunt, P. B., D. I. Robertson, R. D. Bretherton, and R. I. Winton, *SCOOT—A traffic responsive method of coordinating signals*. Transportation Road Research Lab, Crowthorne, U.K., 1981.
- [4] Gartner, N., J. D. Little, and H. Gabbay, *Optimization of traffic signal settings in networks by mixed-integer linear programming*. DTIC Document, 1974.
- [5] Gartner, N. H. and C. Stamatiadis, Arterial-based control of traffic flow in urban grid networks. *Mathematical and computer modelling*, Vol. 35, No. 5, 2002, pp. 657–671.
- [6] Lo, H. K., A novel traffic signal control formulation. *Transportation Research Part A: Policy and Practice*, Vol. 33, No. 6, 1998, pp. 433–448.
- [7] He, Q., K. L. Head, and J. Ding, PAMSCOD: Platoon-based Arterial Multi-modal Signal Control with Online Data. *Procedia-Social and Behavioral Sciences*, Vol. 17, 2011, pp. 462–489.

- [8] Lin, W.-H. and C. Wang, An enhanced 0-1 mixed-integer LP formulation for traffic signal control. *Intelligent Transportation Systems, IEEE Transactions on*, Vol. 5, No. 4, 2004, pp. 238–245.
- [9] Han, K., T. L. Friesz, and T. Yao, A link-based mixed integer LP approach for adaptive traffic signal control. *arXiv preprint arXiv:1211.4625*, 2012.
- [10] Lo, H. K., E. Chang, and Y. C. Chan, Dynamic network traffic control. *Transportation Research Part A: Policy and Practice*, Vol. 35, No. 8, 1999, pp. 721–744.
- [11] He, Q., W.-H. Lin, H. Liu, and K. L. Head, Heuristic algorithms to solve 0–1 mixed integer LP formulations for traffic signal control problems. In *Service Operations and Logistics and Informatics (SOLI), 2010 IEEE International Conference on*, IEEE, 2010, pp. 118–124.
- [12] Smith, S., G. Barlow, X.-F. Xie, and Z. Rubinstein, SURTRAC: Scalable Urban Traffic Control. In *Transportation Research Board 92nd Annual Meeting Compendium of Papers*, Transportation Research Board, 2013.
- [13] Daganzo, C. F., The cell transmission model: A dynamic representation of highway traffic consistent with the hydrodynamic theory. *Transportation Research Part B: Methodological*, Vol. 28, No. 4, 1994, pp. 269–287.
- [14] Daganzo, C. F., The cell transmission model, part II: network traffic. *Transportation Research Part B: Methodological*, Vol. 29, No. 2, 1995, pp. 79–93.
- [15] Xiaojian, H., W. Wei, and H. Sheng, Urban traffic flow prediction with variable cell transmission model. *Journal of Transportation Systems Engineering and Information Technology*, Vol. 10, No. 4, 2010, pp. 73–78.
- [16] Sumalee, A., R. Zhong, T. Pan, and W. Szeto, Stochastic cell transmission model (SCTM): A stochastic dynamic traffic model for traffic state surveillance and assignment. *Transportation Research Part B: Methodological*, Vol. 45, No. 3, 2011, pp. 507–533.
- [17] Jabari, S. E. and H. X. Liu, A stochastic model of traffic flow: Theoretical foundations. *Transportation Research Part B: Methodological*, Vol. 46, No. 1, 2012, pp. 156–174.
- [18] Huang, K. C., *Traffic Simulation Model for Urban Networks: CTM-URBAN*. Ph.D. thesis, Concordia University, 2011.
- [19] Muralidharan, A., G. Dervisoglu, and R. Horowitz, Freeway traffic flow simulation using the link node cell transmission model. In *American Control Conference, 2009. ACC'09.*, IEEE, 2009, pp. 2916–2921.
- [20] Gomes, G. and R. Horowitz, Optimal freeway ramp metering using the asymmetric cell transmission model. *Transportation Research Part C: Emerging Technologies*, Vol. 14, No. 4, 2006, pp. 244–262.
- [21] Kim, Y., *Online traffic flow model applying dynamic flow-density relation*. Int. At. Energy Agency, 2002.

- 1 [22] Lu, S., S. Dai, and X. Liu, A discrete traffic kinetic model—integrating the lagged cell trans-
2 mission and continuous traffic kinetic models. *Transportation Research Part C: Emerging*
3 *Technologies*, Vol. 19, No. 2, 2011, pp. 196–205.
- 4 [23] Alecsandru, C., A. Quddus, K. C. Huang, B. Rouhieh, A. R. Khan, and Q. Zeng, An as-
5 sessment of the cell-transmission traffic flow paradigm: Development and applications. In
6 *Transportation Research Board 90th Annual Meeting*, 2011, 11-1152.